bioengineering

MDPI

Type of the Paper (Article, Review, Communication, etc.)

A Survey on Optical Coherence Tomography – technology and application

Firstname Lastname [1], Firstname Lastname [2] and Firstname Lastname [2,*]

[1] Affiliation 1; e-mail@e-mail.com
[2] Affiliation 2; e-mail@e-mail.com
* Correspondence: e-mail@e-mail.com; Tel.: (optional; include country code; if there are multiple corresponding authors, add author initials)

Abstract: This paper examines research works on Optical Coherence Tomography (OCT). The aim of this paper is to review the progress and efforts of researchers over the past three decades concerning the methods and applications of OCT in medical imaging. This article seeks to pave the way for future research by thoroughly examining existing studies and developments.

Keywords: OCT, Biomedical Imaging, clinical application, Artificial Intelligence

1. Introduction

In the early 1990s, OCT developed into a revolutionary imaging procedure in medical diagnostics. By harnessing the power of near-infrared light, OCT provides high-resolution cross-sectional views of tissues and enables detailed, non-invasive examinations. This capability has proven to be particularly valuable in ophthalmology as it aids in the diagnosis and treatment of various eye diseases. With ongoing advances, the use of OCT is expanding into other medical fields, including dermatology, cardiology and oncology, opening new avenues for understanding disease mechanisms and evaluating treatment outcomes. This article looks at the basic principles, recent advances and increasing applications of OCT, highlighting its growing importance in healthcare.

Over the first two decades of its application, OCT has predominantly been employed for the imaging of ocular tissues [1-8]. This extensive utilization reflects the technology's pivotal role in advancing eye-related diagnostics. Most of the research papers presented in the practical application of OCT have been utilized for imaging results of ocular tissues.

The first reason for this focus stems from the limited penetration depth of light in tissue, typically ranging from one to three millimeters, making OCT alone unsuitable for imaging tissues with significant thickness.

The second reason involves the need for a linear scan of the tissue slice, which necessitates moving the optical fiber or waveguide along the line. Due to the required nanometric resolution, precise robotic arms are essential, generally leading to time inefficiency. However, most methods employ a movable reflective mirror, significantly enhancing the scanning speed [9]. Though at the expense of needing substantial space to accommodate the mechanical equipment for mirror movement. Consequently, these devices must be positioned outside the patient's body, which, given the specific condition of the eye and the transparency of intraocular fluid, is suitable for ocular imaging.

However, in recent years, the concurrent use of ultrasound and OCT imaging, or the employment of rapid robots and transparent tubes, has enabled the visualization of thicker tissues, thereby expanding the possibilities for medical imaging[10,11].

This paper is organized into 7 chapters. Chapter 1 introduces the topic. Chapter 2 outlines the history of development. Chapter 3 discusses the technical foundations and mechanisms. Chapter 4 describes results from applications in OCT. Chapter 5 addresses

Citation: To be added by editorial staff during production.

Academic Editor: Firstname Lastname

Received: date
Revised: date
Accepted: date
Published: date

challenges and limitations. Chapter 6 explores future work and development prospects. Chapter 7 concludes the paper.

2. History and Development

In this chapter, a few important and highly cited articles in the field of OCT that have been published since the beginning are discussed. To become more familiar with the subject literature.

OCT was first introduced in the early 1990s by Huang et al. [12]. OCT is a groundbreaking imaging technique that uses low-coherence light to capture micrometer-resolution, cross-sectional images of biological tissues. This non-invasive method is analogous to ultrasound imaging but employs light instead of sound waves, making it particularly useful for imaging the retina and other ocular structures, as well as for identifying the composition of arterial plaques, which is critical for assessing cardiovascular health.

The authors detail the development and potential applications of OCT, emphasizing its high spatial resolution and sensitivity. The system utilizes a fiber optic Michelson interferometer with a super luminescent diode as the light source, which allows for the detection of backscattered light from within tissues. The technique's ability to differentiate between various tissue types and to image through scattering media makes it a powerful tool for both medical research and clinical diagnosis.

In summary, Huang et al. introduce OCT as a transformative diagnostic technique with the capability to image internal biological structures with unprecedented detail, without the need for invasive procedures. The technology has since become an essential tool in ophthalmology and is expanding into other medical fields, revolutionizing the way clinicians visualize and understand the anatomy and pathology of various diseases.

Then in November 1993, a paper was presented by Swanson et al. [13], which was among one of the first applications of OCT for real imaging. This paper presents the development and demonstration of the first high-speed, micrometer-resolution OCT system for in vivo transpupillary measurements of the human retina. The system uses a super luminescent diode source at ~843 nm with a power of ~175 μW, adhering to safety standards (ANSI Z136). It achieves a longitudinal resolution of ~14 μm and a scanning speed of 160 mm/s, which is four times faster than previously reported results. The integration of the OCT system with a standard ophthalmic slit-lamp biomicroscope allows for precise two-dimensional retinal imaging.

The researchers demonstrate the clinical relevance of OCT by presenting high-resolution tomographs of the retina, including images of the macular region and the optic nerve head. These images reveal intricate retinal structures such as the retinal nerve fiber layer (RNFL), choroid, and optic disk profile. The article also discusses image processing techniques to correct motion artifacts, which are essential for in vivo measurements.

The potential applications of OCT in diagnosing and monitoring retinal diseases are highlighted, including macular degeneration, macular hole, macular edema, and glaucoma. The capability of OCT to provide objective, direct measurements of RNFL thickness could be a significant advancement in early diagnosis and treatment.

In summary, the article showcases OCT as a promising diagnostic technique for non-contact, noninvasive, micrometer-resolution imaging of retinal structure. The system's ability to acquire images in less than 3 seconds, with real-time updating, suggests its clinical feasibility for a variety of retinal imaging applications. The research was supported by various U.S. government and health organizations.

In another work presented by Hee et al. [14], a similar application is shown for imaging the retina of the human eye. The study, conducted in a research laboratory, involved a convenience sample of normal human subjects to validate the correlation between OCT images and known retinal anatomy. The OCT system utilizes a super luminescent diode source and a fiberoptic Michelson interferometer to gather depth information from the retina. The system is sensitive enough to detect weakly reflected light, enabling the creation of detailed tomographic images.

Results indicated that OCT can clearly delineate morphological features of the fovea, optic disc, and the layered structure of the retina with a depth resolution of 10 μm. It can also identify normal variations in retinal and retinal nerve fiber layer (RNFL) thicknesses. The conclusion is that OCT is a promising technique for high-resolution examination of the fundus, which could be beneficial for early diagnosis and monitoring of retinal diseases such as glaucoma, macular degeneration, and macular edema.

The document also elaborates on the materials and methods used in the OCT examination, including the design of the OCT scanner, the examination protocol, and image processing techniques. The OCT examination protocol involves the use of a slit-lamp biomicroscope with a condensing lens to focus the OCT probe beam onto the retina. Image processing techniques include displaying cross-sectional tomographs of the retina in false-color and correcting for motion artifacts.

Several types of OCT scans were performed to highlight normal anatomic variations and potential clinical applications. These include scans along the papillomacular axis, serial sagittal tomographs through the macula, radial tomographs through the optic disc, and circular tomographs in the peripapillary region. These scans demonstrate OCT's ability to profile normal anatomic variations in retinal thickness and to document changes in the nerve fiber layer, which could be crucial for diagnosing and monitoring diseases like glaucoma.

In conclusion, the document presents OCT as a high-resolution imaging technique for the human retina with the potential to significantly advance the diagnosis and management of retinal diseases. It provides a thorough explanation of the technology's capabilities, implementation, and potential impact on the field of ophthalmology.

In one of the most highly cited papers presents a novel deep learning architecture, CE-Net (Context Encoder Network), proposed by Zaiwang Gu et al. [15], for enhancing 2D medical image segmentation. The authors address the issue of spatial information loss in medical image segmentation by developing a network that effectively captures high-level semantic features while preserving spatial details. The CE-Net architecture is composed of three primary modules: a feature encoder module leveraging a pretrained ResNet block, a context extractor module featuring a dense atrous convolution block and a residual multi-kernel pooling block, and a feature decoder module.

The effectiveness of CE-Net is validated through extensive experiments across multiple medical image segmentation tasks, such as optic disc segmentation, retinal vessel detection, lung segmentation, cell contour segmentation, and retinal OCT layer segmentation. The results indicate that CE-Net surpasses existing methods, including the original U-Net and other state-of-the-art approaches, in terms of segmentation accuracy.

An ablation study is conducted to evaluate the contribution of each component of CE-Net to its performance, confirming the significance of the proposed architecture's design. The authors suggest that CE-Net is a versatile and effective solution for 2D medical image segmentation tasks, with potential applications in 3D data segmentation as future work.

In another work by Fang et al. [16], presents a novel deep learning approach, the Lesion-Aware Convolutional Neural Network (LACNN), for the classification of retinal OCT images to enhance the diagnosis of macular diseases. The LACNN integrates a lesion detection network (LDN) to generate attention maps, which guide the classification network to focus on local lesion features, thereby improving the accuracy and efficiency of OCT image classification. The method was validated on two clinical OCT datasets, showing its effectiveness over traditional machine learning and other deep learning methods. The LACNN achieves high performance even with a limited number of training samples, making it a promising tool for computer-aided diagnosis of retinal diseases. The authors suggest that the LACNN framework could be extended to other complex macular diseases, indicating potential areas for future research.

In another highly cited paper, Fang et al. [17], presents a novel Segmentation Based Sparse Reconstruction (SSR) method for enhancing the quality of OCT images, with a

focus on retinal OCT. The SSR method integrates automatic layer segmentation to construct layer-specific structural dictionaries, which are utilized to improve the efficacy of sparsity-based image reconstruction algorithms. The approach is designed to preserve anatomical and pathological features within each layer and to expedite the search for similar patches by restricting it to within segmented layers.

The introduction outlines the difficulties encountered in analyzing OCT images due to noise and low spatial sampling rates, which can be mitigated through effective denoising and interpolation techniques. The document provides a review of various reconstruction models, including traditional spatial domain methods, transform-based methods, and sparse representation models inspired by the human visual system. It also discusses nonlocal sparse reconstruction models that enhance reconstruction by leveraging self-similarities across the image.

The SSR method is composed of three primary components: layer segmentation employing a graph-based algorithm, layer segmentation-based dictionary construction, and layer segmentation-based sparse reconstruction. The method is tailored to maintain the integrity of anatomical and pathological structures within each layer and to accelerate the process of searching for similar patches by confining it within segmented layers.

Experimental results, obtained from clinical OCT data, demonstrate that the SSR method surpasses several state-of-the-art denoising and interpolation methods in terms of quantitative metrics such as PSNR, MSR, and CNR. Additionally, the method exhibits computational efficiency, requiring less computational time than non-local based denoising approaches.

In conclusion, the SSR method is proposed as a versatile technique that can be applied to enhance image quality across a range of tissues and imaging modalities. The authors express gratitude to the A2A Ancillary SDOCT Study group for providing the OCT image dataset used in their experiments.

3. Technical basis and mechanisms

An OCT device consists of three main components: optical, electronic, and software.

Optical part

The optical section of an OCT device is composed of five elements: the light source, splitter, reflector, the tissue under test, and the sensor.

Light source

Typically, an SLD (Superluminescent Diode) is used as the light source in an OCT device. SLDs generate light with low coherence, which implies a high frequency bandwidth and short coherence length. The high bandwidth of the light source helps to eliminate ambiguity in distance measurement[18-20].

Splitter

The splitter typically has two functions: firstly, it divides the emitted light into two parts, and secondly, it combines the two reflected beams of light. Splitters are usually made from transparent materials such as glass or plastic[21-23].

Reflector

The reflector or mirror is responsible for reflecting light. Mirrors should be made from materials that have the capability to reflect light in the desired spectrum for OCT (usually near-infrared). Common materials include aluminum, silver, and certain specialized alloys that are coated with anti-scratch and protective layers to enhance durability and performance under environmental conditions[24,25].

Tissue under test

This section includes the living tissue that is being examined.

Sensor

Photodetector sensors or interferometric cameras are used as sensors in OCT devices. These sensors capture the light that has interacted with the sample and the reference beam, facilitating the interference pattern analysis essential for constructing high-resolution images of the tissue[26,27].

OCT optical part operates based

The operational principles of OCT function as follows: Light is emitted by a light source and this emitted light enters a beam splitter, which divides it into two distinct optical paths. One beam is directed towards a reference mirror, while the other beam is directed towards the tissue under examination. The light that is reflected back from both the mirror and the tissue re-enters the beam splitter where the two beams are recombined. This recombination leads to interference, and the resulting interference pattern is then projected onto a detector or sensor, enabling the acquisition of depth-resolved images.

Physical and Quantitative Examination of Operations

The stages that have been described so far represent a simplified qualitative operation that forms the foundation of OCT. However, to implement OCT, it is necessary to understand the quantitative physical relationships, which are further discussed in the subsequent sections.

The optical path difference between the sample and reference paths is crucial for creating the necessary interference shown in equation (1) [28]. where n is the refractive index of the medium through which light travels, and d is the optical path length traveled by the light within the medium.

$$OPT = 2(n.d) \quad (1)$$

The intensity of the interference light detected can be described by the interference equation shown in equation (2) [29]. where I_1 and I_2 are the intensities of the light reflected from the sample and reference paths, respectively, and $\Delta\emptyset$ is the phase difference between the two light waves.

$$I = I_1 + I_2 + 2\sqrt{I_1 I_2}\cos(\Delta\emptyset) \quad (2)$$

Axial resolution, which determines the imaging accuracy in the depth direction, is calculated as equation (3) [28]. where n is the refractive index of the medium.

$$Axial\ Resolution = \frac{\lambda^2}{2n\Delta\lambda} \quad (3)$$

Lateral resolution is dependent on the diameter of the focused light spot and can be calculated using equation (4) [29]. where NA is the Numerical Aperture of the optical system.

$$Lateral\ Resolution = \frac{0.61\cdot\lambda}{NA} \quad (4)$$

In Figure 1, a simple schematic of OCT optical part is presented.

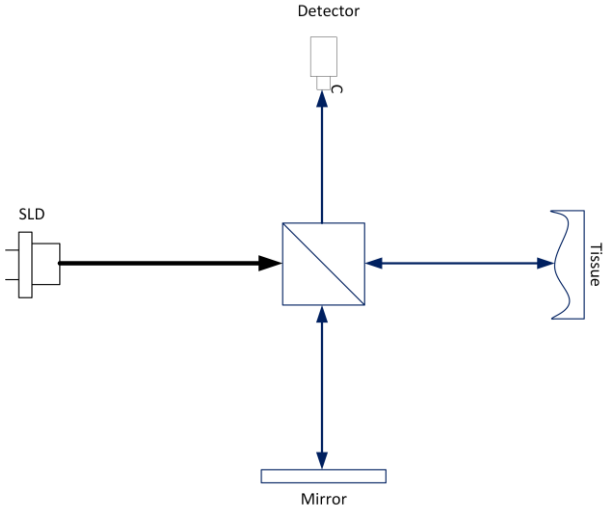

Figure 1 a simple schematic of OCT optical part

Electronic

The electronics component plays a vital role in processing optical signals and converting them into digital images. This section encompasses several key components, each with specific functions. Below is a detailed explanation of these components and their operations:

Detectors

In OCT, detectors are typically photodiodes or other types of photodetectors that convert light into electrical signals. This conversion is facilitated by the photoelectric effect and constitutes the operational foundation of the device[26,27].

Amplifiers

The electrical signals generated by the detectors are generally weak and require amplification. Amplifiers serve this role by strengthening the signals sufficiently for analysis by the central processing system[30].

Filters

Filters are used to eliminate noise and enhance the quality of electrical signals. These components help remove undesirable frequencies or background noises, significantly improving the accuracy of the final image[31].

Analog-to-Digital Converters (ADCs)

After amplification, the signals need to be converted into a digital format to be processed by computers. Analog-to-digital converters perform this transformation, enabling advanced digital processing and data analysis[31,32].

Control System

The control system in OCT is used for managing device settings, coordinating the movement of mechanical components (such as scanning mirrors), and adjusting imaging parameters. This system may also include software for data analysis and image generation[33,34].

Processor

Signal processing, data processing, and user interface tasks are performed with the aid of the processing unit[35,36].

These electronic components in an OCT system collaborate to enable precise and low-noise imaging of biological tissues, ultimately aiding in medical diagnostics. The integration of these components ensures that OCT can provide high-resolution, real-time images that are essential for clinical and research applications.

Software

The software is responsible for comprehensive signal processing, which includes the extraction of A-scan images, the assembly of these images into B-scan images, and further synthesis into three-dimensional C-scan images. Ultimately, artificial intelligence algorithms are employed to process the derived images, ensuring that both the images and analytical results are efficiently transmitted to the user.

Signal processing

Extracted digital data are fed into the processor, where signal processing operations are performed on these data. Initially, the data enter a preprocessing stage where noise levels are corrected using filters. Subsequently, the main processing, which is the Fourier Transform, will be performed on the data. The Fourier Transform is essential for converting overlapping signals into spatial data. The use of the Fast Fourier Transform (FFT) is crucial as it enables the observation and analysis of the amplitude and phase of signals in frequency space[37,38].

A-scan

The results from the Fourier Transform are displayed in a graph, where the horizontal axis represents depth and the vertical axis represents signal intensity. This graph aids in the precise localization of structures within the sample.

B-scan

To produce a B-scan image, the optical scanner moves laterally across the sample, generating an image line (A-scan) at each point. These consecutive lines are joined together to form a two-dimensional image.

C-scan

To form a three-dimensional image, or C-scan, one can achieve this by assembling consecutive B-scans together.

AI algorithms

Artificial intelligence can provide substantial assistance in the following scenarios. Automated Disease Diagnosis, Image Quality Improvement, Fast and Accurate Analysis, Process Automation and Prediction and Prevention[39-41].

Various types of OCT

The described structure is merely a simplified model of OCT; actual models possess many complexities. For example, OCT can be categorized into various types based on structural differences. Below are some of these types.

Time Domain OCT (TD-OCT)

TD-OCT works by measuring the time delay of light reflected from different depths within the sample using a reference mirror and a low-coherence light source. TD-OCT can differentiate layers within the retina, aiding in the diagnosis of conditions like glaucoma and macular degeneration [42].

Spectral Domain OCT (SD-OCT)

SD-OCT is using a broadband light source and a spectrometer. Unlike TD-OCT, SD-OCT measures the interference spectrum of reflected light, allowing for faster image acquisition and improved resolution. This technology is particularly useful in ophthalmology for examining the retina and diagnosing conditions like macular degeneration and diabetic retinopathy. SD-OCT's ability to provide real-time, high-resolution images makes it a valuable tool in clinical practice [43,44].

Swept Source OCT (SS-OCT)

SS-OCT uses a tunable laser source to capture high-speed and high-resolution cross-sectional images of biological tissues. By sweeping the laser across a range of wavelengths, SS-OCT collects depth information more quickly than traditional methods. This technology is particularly beneficial in ophthalmology, enabling detailed visualization of the retina and choroid, and is effective in diagnosing and managing eye diseases like glaucoma and age-related macular degeneration. SS-OCT's extended imaging depth and speed make it suitable for a wide range of clinical applications [45,46].

Fourier Domain Mode Locked OCT (FDML OCT)

FDML OCT is an advanced imaging technique that utilizes a FDML laser to achieve high-speed and high-resolution imaging. FDML lasers enable rapid wavelength sweeping, allowing for fast acquisition of OCT images without the need for resampling in the frequency domain. This technology significantly enhances imaging speed and depth range, making it particularly useful in medical imaging applications such as ophthalmology. FDML OCT provides detailed cross-sectional images of tissues, aiding in the diagnosis and monitoring of various conditions. The combination of high speed and resolution makes FDML OCT a valuable tool for real-time imaging applications [47-49].

4. Application

In this section, we focus on practical papers in the field of Optical Coherence Tomography (OCT), examining their applications, results, and obtained outcomes.

In the study conducted by Gardecki et al., micro-OCT is presented [50]. μOCT offers high-resolution imaging of prostate tissue, capable of resolving architectural and cellular features associated with benign and neoplastic prostate conditions. The μOCT system uses a spectral-domain OCT with a broad bandwidth light source, achieving an axial resolution of less than 1 μm. Despite its penetration depth of 300-500 μm, which is greater than other in vivo microscopy modalities, it remains insufficient for imaging the entire prostate with a realistic number of needle insertions. The study suggests that imaging at longer wavelengths could significantly increase penetration depth, potentially doubling or tripling current values. Implementing μOCT in a small-diameter probe for in vivo use could reduce biopsy sampling errors and enhance prostate cancer diagnosis. The study found that 14% of the samples contained prostate cancer, while 86% were benign, indicating μOCT's potential utility in prostate diagnostics.

In another study conducted by Zhou et al., the research focused on detecting early-stage degeneration of human articular cartilage using polarization-sensitive OCT (PS-OCT) [51]. The study demonstrates the efficacy of PS-OCT in differentiating bone tissue types, particularly in the context of prostate cancer-associated bone metastases (PCBM). The degree of ordered organization (DOO) feature, derived from PS-OCT, effectively distinguishes between trabecular and irregular bone regions, offering a non-invasive alternative to traditional imaging methods. The integration of PS-OCT with MATLAB-based image analysis tools allows for detailed examination of bone microstructures, such as lacunae morphology, at a rapid pace, enhancing the efficiency of research cycles. Despite its potential, the study acknowledges the sensitivity of PS-OCT to environmental conditions and the need for further development for in-vivo applications. The combination of PS-OCT with conventional techniques like CT and SEM provides a comprehensive understanding of bone tissue dynamics, paving the way for advancements in bone-related pathologies. Future work aims to develop a fiber-based endoscope for in-vivo imaging, potentially expanding the clinical utility of PS-OCT.

In the paper presented by Waheed et al. [52], OCT-Angiography (OCTA) has emerged as a pivotal tool in the assessment of diabetic retinopathy (DR), offering detailed insights into retinal microvascular changes. The technology's ability to visualize and quantify the foveal avascular zone (FAZ) and vessel density provides critical data for evaluating DR severity and progression. Despite its potential, challenges such as image artifacts and variability in FAZ metrics remain, necessitating further refinement in imaging techniques and standardization across studies. Recent advancements in OCTA, including higher-speed platforms and improved software, are enhancing the precision of peripheral retina assessments, crucial for detecting neovascularization and non-perfusion. These developments underscore OCTA's role in advancing our understanding of DR and supporting the development of new therapeutic strategies. Future research should focus on correlating OCTA metrics with visual function to validate their clinical utility.

In another work presented by Azzollini et al. [53], Dynamic-OCT (D-OCT) is a cutting-edge imaging technique that provides label-free, live optical imaging of dynamic cellular and subcellular features by analyzing temporal fluctuations of optical signals associated with intracellular organelle movements. This method offers insights into cellular physiology and is particularly promising for three-dimensional evaluation of live tissue samples, such as freshly excised biopsies and 3D cell cultures. D-OCT leverages the temporal behavior of optical signals to gain deeper insights into cellular mechanisms, allowing for the visualization of specific cells and their nuclei, and identifying cell mitotic states. It circumvents the need for fluorescent dyes, thus avoiding photo-toxicity and biases introduced by fluorescent markers. Applications of D-OCT include monitoring cell states, detecting apoptosis, and assessing responses to anti-cancer drugs in vitro. It is also used

for ex vivo tissue analysis, such as detecting different tissue components and changes in OCT signal variance due to lipid droplet movements.

Huang et al. presented a needle-based OCT with real time visualization capabilities [54]. The study investigated the use of Needle-Probe OCT for real-time visualization of Veress needle placement in a porcine model, aiming to enhance the safety of pneumoperitoneum establishment in laparoscopic surgery. The primary outcome was a 97.5% success rate in peritoneal punctures, with no intra-abdominal organ injuries reported. The OCT system transformed the traditionally blind closed technique into a visualized procedure, improving the safety of peritoneal access. Statistical analysis showed a significant difference in the standard deviation (STD) of OCT images, indicating high discrimination capability between the peritoneum and extra-peritoneal tissue, with an area under the ROC curve (AUC) of 0.97. The study suggests that the OCT system could be a valuable tool for minimally invasive procedures in modern surgery. Additionally, 74.7% of surveyed surgeons expressed willingness to use the Veress needle again if an assisted device could visualize the puncturing process.

In another reported work by Kuo et al. [55], highlights the effectiveness of the Quadratic Support Vector Machine (QSVM) classifier in identifying the epidural space (ES) with high sensitivity (97.5%), specificity (95%), and accuracy (96.2%). The OCT needle probe, integrated with machine learning, provides real-time, high-resolution imaging for accurate needle placement in medical procedures, particularly in neuraxial blocks. The handheld OCT needle probe, although currently limited to larger needles, offers potential for compact and cost-effective clinical applications. The system's ability to provide detailed anatomical imaging from the needle tip complements ultrasound-guided methods, although it does not guide the needle's trajectory. The OCT technology is also explored for other medical applications, such as fascial blocks, emphasizing the need for further validation in clinical practice. The integration of OCT with artificial intelligence presents an opportunity to improve the quality of medical care amidst increasing demand and limited human resources.

5. Challenges and Limitations

In this part I am going to describe the limitations that we understood until now.

6. Future and Development

To describe some Ideas for our work

7. Conclusion

References

1. Fercher, A.F.; Hitzenberger, C.K.; Kamp, G.; El-Zaiat, S.Y. Measurement of intraocular distances by backscattering spectral interferometry. *Optics Communications* **1995**, *117*, 43-48, doi:https://doi.org/10.1016/0030-4018(95)00119-S.
2. Drexler, W.; Morgner, U.; Kärtner, F.; Pitris, C.; Boppart, S.; Li, X.; Ippen, E.; Fujimoto, J. In vivo ultrahigh-resolution optical coherence. *Opt. Lett.* **1999**, *24*, 1221-1223, doi:10.1364/OL.24.001221.
3. Wojtkowski, M.; Leitgeb, R.; Kowalczyk, A.; Bajraszewski, T.; Fercher, A. In vivo human retinal imaging by Fourier Domain optical coherence tomography. *Journal of biomedical optics* **2002**, *7*, 457-463, doi:10.1117/1.1482379.
4. Nassif, N.; Cense, B.; Park, B.; Pierce, M.; Yun, S.; Bouma, B.; Tearney, G.; Chen, T.; Boer, J. In vivo high-resolution video-rate spectral-domain optical coherence tomography of the human retina and optic nerve. *Optics express* **2004**, *12*, 367-376, doi:10.1364/OPEX.12.000367.
5. Scholda, C.; Wirtitsch, M.; Hermann, B.; Unterhuber, A.; Ergun, E.; Sattmann, H.; Ko, T.; Fujimoto, J.; Fercher, A.; Stur, M.; et al. Ultrahigh resolution optical coherence tomography of macular holes. *Retina (Philadelphia, Pa.)* **2006**, *26*, 1034-1041, doi:10.1097/01.iae.0000254898.80552.e7.
6. Potsaid, B.; Baumann, B.; Huang, D.; Barry, S.; Cable, A.; Schuman, J.; Duker, J.; Fujimoto, J. Ultrahigh speed 1050nm swept source / Fourier domain OCT retinal and anterior segment imaging at 100,000 to 400,000 axial scans per second. *Optics express* **2010**, *18*, 20029-20048, doi:10.1364/OE.18.020029.
7. Jia, Y.; Tan, O.; Tokayer, J.; Potsaid, B.; Wang, Y.; Liu, J.; Kraus, M.; Molly Subhash, H.; Fujimoto, J.; Hornegger, J.; et al. Split-spectrum amplitude-decorrelation angiography with optical coherence tomography. *Optics Express* **2012**, *20*, 4710-4725, doi:10.1364/OE.20.004710.
8. Zhang, Y.; Cense, B.; Rha, J.; Jonnal, R.S.; Gao, W.; Zawadzki, R.J.; Werner, J.S.; Jones, S.; Olivier, S.; Miller, D.T. High-speed volumetric imaging of cone photoreceptors with adaptive optics spectral-domain optical coherence tomography. *Optics Express* **2006**, *14*, 4380-4394, doi:10.1364/OE.14.004380.
9. Chinn, S.R.; Swanson, E.A.; Fujimoto, J.G. Optical coherence tomography using a frequency-tunable optical source. *Opt. Lett.* **1997**, *22 5*, 340-342.
10. Muller, B.G.; Swaan, A.; de Bruin, D.M.; van den Bos, W.; Schreurs, A.W.; Faber, D.J.; Zwartkruis, E.C.; Rozendaal, L.; Vis, A.N.; Nieuwenhuijzen, J.A.; et al. Customized Tool for the Validation of Optical Coherence Tomography in Differentiation of Prostate Cancer. *Technol Cancer Res Treat* **2017**, *16*, 57-65, doi:10.1177/1533034615626614.
11. Swaan, A.; Mannaerts, C.K.; Muller, B.G.; van Kollenburg, R.A.; Lucas, M.; Savci-Heijink, C.D.; van Leeuwen, T.G.; de Reijke, T.M.; de Bruin, D.M. The First In Vivo Needle-Based Optical Coherence Tomography in Human Prostate: A Safety and Feasibility Study. *Lasers Surg Med* **2019**, *51*, 390-398, doi:10.1002/lsm.23093.
12. Huang, D.; Swanson, E.A.; Lin, C.P.; Schuman, J.S.; Stinson, W.G.; Chang, W.; Hee, M.R.; Flotte, T.; Gregory, K.; Puliafito, C.A.; et al. Optical coherence tomography. *Science* **1991**, *254*, 1178-1181, doi:10.1126/science.1957169.
13. Swanson, E.A.; Izatt, J.A.; Lin, C.P.; Fujimoto, J.G.; Schuman, J.S.; Hee, M.R.; Huang, D.; Puliafito, C.A. In vivo retinal imaging by optical coherence tomography. *Opt. Lett.* **1993**, *18*, 1864-1866, doi:10.1364/OL.18.001864.
14. Hee, M.R.; Izatt, J.A.; Swanson, E.A.; Huang, D.; Schuman, J.S.; Lin, C.P.; Puliafito, C.A.; Fujimoto, J.G. Optical Coherence Tomography of the Human Retina. *Archives of Ophthalmology* **1995**, *113*, 325-332, doi:10.1001/archopht.1995.01100030081025.
15. Gu, Z.; Cheng, J.; Fu, H.; Zhou, K.; Hao, H.; Zhao, Y.; Zhang, T.; Gao, S.; Liu, J. CE-Net: Context Encoder Network for 2D Medical Image Segmentation. *IEEE Transactions on Medical Imaging* **2019**, *38*, 2281-2292, doi:10.1109/TMI.2019.2903562.
16. Fang, L.; Wang, C.; Li, S.; Rabbani, H.; Chen, X.; Liu, Z. Attention to Lesion: Lesion-Aware Convolutional Neural Network for Retinal Optical Coherence Tomography Image Classification. *IEEE Transactions on Medical Imaging* **2019**, *38*, 1959-1970, doi:10.1109/TMI.2019.2898414.

17. Fang, L.; Li, S.; Cunefare, D.; Farsiu, S. Segmentation Based Sparse Reconstruction of Optical Coherence Tomography Images. *IEEE Transactions on Medical Imaging* **2017**, *36*, 407-421, doi:10.1109/TMI.2016.2611503.
18. Shu, X.; Beckmann, L.; Zhang, H. Visible-light optical coherence tomography: a review. *J Biomed Opt* **2017**, *22*, 1-14, doi:10.1117/1.Jbo.22.12.121707.
19. Shidlovski, V.R. Superluminescent Diode Light Sources for OCT. In *Optical Coherence Tomography: Technology and Applications*, Drexler, W., Fujimoto, J.G., Eds.; Springer Berlin Heidelberg: Berlin, Heidelberg, 2008; pp. 281-299.
20. Ozaki, N.; Childs, D.; Sarma, J.; Roberts, T.; Yasuda, T.; Shibata, H.; Ohsato, H.; Watanabe, E.; Ikeda, N.; Sugimoto, Y.; et al. Superluminescent diode with a broadband gain based on self-assembled InAs quantum dots and segmented contacts for an optical coherence tomography light source. *Journal of Applied Physics* **2016**, *119*, 083107, doi:10.1063/1.4942640.
21. Akca, B.I.; Považay, B.; Alex, A.; Wörhoff, K.; de Ridder, R.M.; Drexler, W.; Pollnau, M. Miniature spectrometer and beam splitter for an optical coherence tomography on a silicon chip. *Optics Express* **2013**, *21*, 16648-16656, doi:10.1364/OE.21.016648.
22. Sharma, B.; Kishor, K.; Sharma, S.; Makkar, R. Design and Simulation of Broadband Beam Splitter on a Silicon Nitride Platform for Optical Coherence Tomography. *Fiber and Integrated Optics* **2019**, *38*, 247-257, doi:10.1080/01468030.2019.1639001.
23. Heemskerk, E.; Akca, B.I. On-chip polarization beam splitter design for optical coherence tomography. *Optics Express* **2018**, *26*, 33349-33355, doi:10.1364/OE.26.033349.
24. Pandiyan, V.P.; Jiang, X.; Kuchenbecker, J.A.; Sabesan, R. Reflective mirror-based line-scan adaptive optics OCT for imaging retinal structure and function. *Biomed. Opt. Express* **2021**, *12*, 5865-5880, doi:10.1364/BOE.436337.
25. Singh, K.; Reddy, R.; Sharma, G.; Verma, Y.; Gardecki, J.A.; Tearney, G. In-line optical fiber metallic mirror reflector for monolithic common path optical coherence tomography probes. *Lasers Surg Med* **2018**, *50*, 230-235, doi:10.1002/lsm.22756.
26. Yurtsever, G.; Považay, B.; Alex, A.; Zabihian, B.; Drexler, W.; Baets, R. Photonic integrated Mach-Zehnder interferometer with an on-chip reference arm for optical coherence tomography. *Biomed. Opt. Express* **2014**, *5*, 1050-1061, doi:10.1364/BOE.5.001050.
27. Girshovitz, P.; Shaked, N.T. Doubling the field of view in off-axis low-coherence interferometric imaging. *Light: Science & Applications* **2014**, *3*, e151-e151, doi:10.1038/lsa.2014.32.
28. Drexler, W.; Fujimoto, J.G. *Optical Coherence Tomography: Technology and Applications*; Springer Berlin Heidelberg: 2008.
29. Brezinski, M.E. *Optical Coherence Tomography: Principles and Applications*; Elsevier Science: 2006.
30. Xu, W.; Mathine, D.; Barton, J. Analog CMOS Design for Optical Coherence Tomography Signal Detection and Processing. *IEEE transactions on bio-medical engineering* **2008**, *55*, 485-489, doi:10.1109/TBME.2007.905402.
31. Frosz, M.; Juhl, M.; Lang, M. Optical Coherence Tomography: System Design and Noise Analysis. **2001**.
32. Ambekar, Y.; Singh, M.; Schill, A.; Zhang, J.; Zevallos Delgado, C.; Khajavi, B.; Aglyamov, S.; Finnell, R.; Scarcelli, G.; Larin, K. Multimodal imaging system combining optical coherence tomography and Brillouin microscopy for neural tube imaging. *Opt. Lett.* **2022**, *47*, 1347-1350, doi:10.1364/OL.453996.
33. Ahronovich, E.Z.; Simaan, N.; Joos, K.M. A Review of Robotic and OCT-Aided Systems for Vitreoretinal Surgery. *Adv Ther* **2021**, *38*, 2114-2129, doi:10.1007/s12325-021-01692-z.
34. Baran, Y.; Rabenorosoa, K.; Laurent, G.; Rougeot, P.; Andreff, N.; Brahim, T. *Preliminary results on OCT-based position control of a concentric tube robot*; 2017; pp. 3000-3005.
35. Ma, Z.; He, Z.; Wang, S.; Wang, Y.; Mengchao, L.; Wang, Q.; Lv, J.; Wang, F. Practical approach for dispersion compensation in spectral-domain optical coherence tomography. *Optical Engineering* **2012**, *51*, 3203, doi:10.1117/1.OE.51.6.063203.
36. Liu, X.; Shao, W.; Wu, K.; Lin, L. The DSP-based data acquisition and processing system for OCT. *Proceedings of SPIE - The International Society for Optical Engineering* **2002**, doi:10.1117/12.482930.
37. Ali, M.; Parlapalli, R. Signal Processing Overview of Optical Coherence Tomography Systems for Medical Imaging. *Texas Instrum.* **2010**.

38. Schaefer, A.W.; Reynolds, J.J.; Marks, D.L.; Boppart, S.A. Real-time digital signal processing-based optical coherence tomography and Doppler optical coherence tomography. *IEEE Trans Biomed Eng* **2004**, *51*, 186-190, doi:10.1109/tbme.2003.820369.
39. Bai, J.; Wan, Z.; Li, P.; Chen, L.; Wang, J.; Fan, Y.; Chen, X.; Peng, Q.; Gao, P. Accuracy and feasibility with AI-assisted OCT in retinal disorder community screening. *Front Cell Dev Biol* **2022**, *10*, 1053483, doi:10.3389/fcell.2022.1053483.
40. Muntean, G.A.; Marginean, A.; Groza, A.; Damian, I.; Roman, S.A.; Hapca, M.C.; Muntean, M.V.; Nicoară, S.D. The Predictive Capabilities of Artificial Intelligence-Based OCT Analysis for Age-Related Macular Degeneration Progression-A Systematic Review. *Diagnostics (Basel)* **2023**, *13*, doi:10.3390/diagnostics13142464.
41. Chandramohan, N.; Hinton, J.; O'Kane, P.; Johnson, T.W. Artificial Intelligence for the Interventional Cardiologist: Powering and Enabling OCT Image Interpretation. *Interventional Cardiology 2024;19:e03* **2024**, doi:10.15420/icr.2023.13.
42. Chen, S.; Gao, R.; McAlinden, C.; Ye, J.; Wang, Y.; Chen, M.; Huang, J.; Sun, Y.; Yu, A.Y. Comparison of Anterior Ocular Biometric Measurements Using Swept-Source and Time-Domain Optical Coherence Tomography. *Journal of Ophthalmology* **2020**, *2020*, 9739878, doi:https://doi.org/10.1155/2020/9739878.
43. Schuman, J.S. Spectral domain optical coherence tomography for glaucoma (an AOS thesis). *Trans Am Ophthalmol Soc* **2008**, *106*, 426-458.
44. Chan, V.T.T.; Sun, Z.; Tang, S.; Chen, L.J.; Wong, A.; Tham, C.C.; Wong, T.Y.; Chen, C.; Ikram, M.K.; Whitson, H.E.; et al. Spectral-Domain OCT Measurements in Alzheimer's Disease: A Systematic Review and Meta-analysis. *Ophthalmology* **2019**, *126*, 497-510, doi:10.1016/j.ophtha.2018.08.009.
45. Vira, J.; Marchese, A.; Singh, R.B.; Agarwal, A. Swept-source optical coherence tomography imaging of the retinochoroid and beyond. *Expert Rev Med Devices* **2020**, *17*, 413-426, doi:10.1080/17434440.2020.1755256.
46. Laíns, I.; Wang, J.C.; Cui, Y.; Katz, R.; Vingopoulos, F.; Staurenghi, G.; Vavvas, D.G.; Miller, J.W.; Miller, J.B. Retinal applications of swept source optical coherence tomography (OCT) and optical coherence tomography angiography (OCTA). *Prog Retin Eye Res* **2021**, *84*, 100951, doi:10.1016/j.preteyeres.2021.100951.
47. Huang, D.; Shi, Y.; Li, F.; Wai, P.K.A. Fourier Domain Mode Locked Laser and Its Applications. *Sensors (Basel)* **2022**, *22*, doi:10.3390/s22093145.
48. Huber, R.; Adler, D.C.; Fujimoto, J.G. Buffered Fourier domain mode locking: unidirectional swept laser sources for optical coherence tomography imaging at 370,000 lines/s. *Opt. Lett.* **2006**, *31*, 2975-2977, doi:10.1364/OL.31.002975.
49. Lin, W.; Bijuan, C. Swept source optical coherence tomography system based on Fourier-domain mode-locked (FDML). In Proceedings of the Proc.SPIE, 2024; p. 1317916.
50. Gardecki, J.A.; Singh, K.; Wu, C.-L.; Tearney, G.J. Imaging the Human Prostate Gland Using 1-μm-Resolution Optical Coherence Tomography. *Archives of Pathology & Laboratory Medicine* **2018**, *143*, 314-318, doi:10.5858/arpa.2018-0135-OA.
51. Zhou, C.; Jung, N.; Xu, S.; Eltit-Guersetti, F.; Lu, X.; Wang, Q.; Liang, D.; Morrissey, C.; Corey, E.; True, L.D.; et al. Imaging and quantification of prostate cancer-associated bone by polarization-sensitive optical coherence tomography. *bioRxiv* **2024**, 2024.2002.2021.581336, doi:10.1101/2024.02.21.581336.
52. Waheed, N.K.; Rosen, R.B.; Jia, Y.; Munk, M.R.; Huang, D.; Fawzi, A.; Chong, V.; Nguyen, Q.D.; Sepah, Y.; Pearce, E. Optical coherence tomography angiography in diabetic retinopathy. *Progress in Retinal and Eye Research* **2023**, *97*, 101206, doi:https://doi.org/10.1016/j.preteyeres.2023.101206.
53. Azzollini, S.; Monfort, T.; Thouvenin, O.; Grieve, K. Dynamic optical coherence tomography for cell analysis [Invited]. *Biomed. Opt. Express* **2023**, *14*, 3362-3379, doi:10.1364/BOE.488929.
54. Huang, E.Y.-H.; Kao, M.-C.; Ting, C.-K.; Huang, W.J.S.; Yeh, Y.-T.; Ke, H.-H.; Kuo, W.-C. Needle-Probe Optical Coherence Tomography for Real-Time Visualization of Veress Peritoneal Needle Placement in a Porcine Model: A New Safety Concept for Pneumoperitoneum Establishment in Laparoscopic Surgery. *Biomedicines* **2022**, *10*, 485.

55. Kuo, W.C.; Kao, M.C.; Ting, C.K.; Teng, W.N. Optical Coherence Tomography Needle Probe in Neuraxial Block Application. *IEEE Journal of Selected Topics in Quantum Electronics* **2021**, *27*, 1-6, doi:10.1109/JSTQE.2020.3042076.